Mitochondrial Mutations in Cholestatic Liver Disease with Biliary Atresia

Hong Koh

Department of Medicine

The Graduate School, Yonsei University

Mitochondrial Mutations in Cholestatic Liver Disease with Biliary Atresia

Directed by Professor Kook In Park

The Doctoral Dissertation submitted to the Department of Medicine, the Graduate School of Yonsei University in of partial fulfillment of the requirements for the degree of Doctor of Philosophy

Hong Koh

December 2016

This certifies that the Doctoral Dissertation of Hong Koh is approved.

Thesis Supervisor: Kook In Park

Thesis Committee Member: Si Young Song

Thesis Committee Member: Young Mock Lee

Thesis Committee Member: Kyoung Jin Shin

Thesis Committee Member: Jae Sung Ko

The Graduate School

Yonsei University

December 2016

ACKNOWLEDGEMENTS

First and foremost, I would like to express my great gratitude for Prof. Kook In Park, my supervisor, who permitted me to have a great opportunity to be a PhD course.

I owe a special thanks to Prof. Si Young Song, Prof. Young Mock Lee, Prof. Kyoung Jin Shin, and Prof. Jae Sung Ko who have given special advices for me to follow the right direction on this research. I am obviously very much indebted to all of my colleagues (Prof. JH Shin, Prof. DW Lee, Prof. S Kim, Dr. KS Park and Dr. SM Shin) for giving me this opportunity to study and for providing valuable resources and help conductive to the completion of the thesis.

My special thanks go to my respectable family who constantly provide emotional support and took care of me in many aspects. Last, but not least, I am grateful to my lovely wife Youngsun Jeon for her thoughtful regards and devote this achievement. Thank you very much.

Hong Koh

December 2016

<TABLE OF CONTENTS>

LIST OF FIGURES

LIST OF TABLES

ABSTRACT

Mitochondrial Mutations in Cholestatic Liver Disease with Biliary Atresia

Hong Koh

Department of Medicine

The Graduate School, Yonsei University

(Directed by Professor Kook In Park)

Biliary atresia (BA) typically induces the severe bile blockade due to the absence of extrahepatic ducts for bile drainage. Even after a successful Kasai hepatic portoenterostomy, a fair number of pediatric patients are likely to be progressively worse for their liver functions. Such clinical prognostic features tempted us to investigate the functionality of liver, which is highly associated with mutations in mitochondrial DNA (mtDNA) of hepatocyte. To assess such a conjecture on mitochondrial dysfunctions in liver as the prognosis-causing mechanism, we sequenced the mtDNA genes encoding the respiratory chains in liver specimens from 14 patients with BA and 5 patients in choledochal cyst (CC) using the next generation sequencing technique. Consequently, we found frequent non-synonymous variations in the genes encoding mitochondrial

respiratory chains for all patients we examined. Particularly, BA patients exhibit several single nucleotide polymorphism-like mutations in the complex I, where subunit assembly and proton pumping activity are critical for mitochondrial functionality. Four (BA4, BA7, BA9, and BA12) of fourteen BA patients described here were found to have distinct pathogenic mutations (T119A and I278V) in still another mtDNA protein-coding gene, that for ND2. Hepatic dysfunction as well as liver impairment was severely present in all four patients. Another set of mutations in ND4 of complex I (i.e., Y95H and S97stop) were found in four (BA3, BA8, BA11, and BA14) of BA patients. Those patients' livers were severely fibrotic damaged, whereas there was no other hepatological functional abnormality. In addition, the parameters of acute hepatic injury and liver function for BA patients are significantly correlated with the extent of clinical symptoms in liver disease. Therefore, this study highlights the roles of mitochondrial function in normal hepatocyte physiology and BA disease to elucidate pathological mechanisms associated with mitochondrial dysfunctions.

Key Words: biliary atresia, mitochondrial DNA mutation, respiratory chain complex, next generation sequencing

Mitochondrial Mutations in Cholestatic Liver Disease with Biliary Atresia

Hong Koh

Department of Medicine

The Graduate School, Yonsei University

(Directed by Professor Kook In Park)

I. INTRODUCTION

Cholestasis as the state, that leads to stasis and accumulation of potentially toxic bile acids in the liver and the systemic circulation,[1] can be generated by different causes such as inflammation, viral infection, autoimmune disease, and congenital disorders of the hepatobiliary systems.[2-4] In particular, biliary atresia (BA) is a progressive fibro-inflammatory cholangiopathy of neonates, and the most common cause of cholestatic liver diseases for children whose liver could be subjected to urgent transplantation, otherwise severely fatal. Cholestasis with BA causes a chronic liver disease defined as severe alterations in hepatic morphology and physiology.[5-7] Since chronic liver diseases undergo persistent and massive apoptosis,[8] apoptosis-mediated fibrogenesis, eventually resulting in cirrhosis of the liver, is likely to be tightly associated with mitochondrial

dysfunction in hepatocytes.[9] Indeed, mutations in mitochondrial DNA (mtDNA) can alter the efficiency of cellular energy transduction, resulting in the multisystemic disorders through the mitochondrial dysfunction.[10,11] Such a multisystemic disorder includes several distinct syndromes such as the Reye's syndrome, Wilson's disease, Hereditary hemochromatosis, and Zellweger syndrome.[12] Hence, mitochondria involved in several steps of the progression of the pathology are a key component in the cholestatic liver diseases. The most common cause of liver transplantation in children is BA, and Kasai hepatic portoenterostomy is a surgical treatment performed on infants with BA to allow for bile drainage. Such a procedure, even though not perfectly curative, may relieve jaundice and stop liver fibrosis, allowing normal growth and development. After surgery, bilirubin levels will fall to normal values in about 50-55% of infants allowing 40-50% to retain their own liver to reach the age of 5 and 10 years.[5-7] Liver transplantation is an option for those children whose liver function and symptoms fail to respond to a Kasai operation. Nevertheless, it is not yet known whether such a disorder in hepatic mitochondria is transmitted by nonmendelian, maternal inheritance, or a sporadic condition. Even worse, it is not so evident that cholestatic liver disease is tightly linked and/or associated with mitochondrial dysfunction. Until recently, little was known about the molecular basis of BA as the sole manifestation of mitochondrial dysfunction in patients with sporadic cases.

Mitochondria play an essential role in the production of adenosine triphosphate (ATP) as cellular energy currency and reactive oxygen species (ROS) as signal, pumping of cytosolic Ca^{2+}, and the regulation of apoptosis.[13] Hepatocytes are rich in mitochondria in such a way that each hepatocyte contains about almost thousand mitochondria corresponding to about 18% of the entire cell volume. In particular, many critical metabolic pathways such as gluconeogenesis, oxidation of triacylglycerides,

decomposition of fatty acids, deamination and transamination of amino acids, and the synthesis of most of the plasma proteins are carried out predominantly in hepatocytes.[14,15] Thus, it is evident that impaired function of mitochondria can cause severe damage to hepatocytes in synthesizing molecules that are utilized elsewhere to support homeostasis, in converting molecules of one type to another, and in regulating energy balances.[16-18] Human mtDNA is found in the matrix and consists of 13 structural genes that encode integral membrane subunits for complexes I, III, IV, and V in the mitochondrial respiratory chain. The mitochondrial matrix possesses an incomplete mtDNA repair system, and is highly sensitive to ROS-induced oxidative damage due to its proximity to the inner mitochondrial membrane where most of the ROS are produced.[19-21] Accumulation of toxic bile acids in the liver and systemic circulation negatively affect the mitochondrial function by direct impaired activities of energy transducing complexes involved in the oxidative phosphorylation in liver.[22] In addition, nonfunctional mitochondria are important sources for the production of ROS, which in turn can promote the onset of apoptosis and are responsible for the activation of profibrogenic mechanism.[23,24] Major alterations of energy metabolism in experimental cholestasis resemble metabolic alterations observed in patient with cirrhosis.[25] Part of the adverse effects of bile acids on mitochondrial bioenergetics could be related to the disturbances of mitochondrial membrane composition.[22] Yet, the specific mechanisms involved in the onset and development of human hepatic mitochondrial dysfunction in liver cholestasis still remains unclear.

In this study, using a next-generation sequencing technique, we performed a mitochondrial genome-wide analysis to investigate the extent of mtDNA mutation in the liver of BA patients, particularly focusing on the genes encoding energy transducing components (ETC) involved in the respiratory chain, together with those of livers from

choledochal cyst (CC) patients as a counterpart. For this aim, we describe the fourteen BA patients we have identified and reviewed their characteristics of the five CC patients identified previously. A comparison of clinical, morphologic, biochemical and genetic features of these patients reveals a remarkable uniformity, suggesting that mutations in the mitochondrial genes encoding ETC seem to be highly associated with BA without evidence of maternal inheritance.

II. MATERIALS AND METHODS

1. Patients and clinical characteristics

Nineteen patiens who were newly diagnosed as having BA as a disease group or CC as a control group at Severance Children's Hospital between August 2011 and July 2015, were enrolled. This study was approved by our institutional review board, and study protocol was in accordance with the Declaration of Helsinki. For all of the patients, the demographic and biochemical parameters such as sex, age in weeks, serum aspartate aminotransferase (AST), alanine aminotransferase (ALT), total bilirubin (T.Bil), direct bilirubin (D.Bil), protein, albumin and gamma glutamyl transpeptidase (*r*-GT), were included at the time of liver wedge biopsy during surgery.

2. Collection and qualification of liver tissue

Liver wedge biopsy specimens were collected from the patients at the time of surgery (Kasai hepatic portoenterostomy or liver transplantation in BA group, choledochojejunostomy with a Roux-en-Y anastomosis of dilated bile duct in CC group). All liver tissues were frozen and stored in liquid nitrogen immediately. For qualification of liver tissues of BA as a disease group and CC as a control group, liver fibrosis and necroinflammatory activity of each group were evaluated according to the METAVIR scoring system.[26] The METAVIR scoring system consists of 5 stages, based on the architectural features of portal fibrosis: F0 = normal, F1 = portal fibrosis without septa, F2 = portal fibrosis and few septa, F3 = numerous septa without cirrhosis, and F4 = cirrhosis.[27,28]

3. Liver tissue mitochondria and mitochondrial DNA extraction

Mitochondria were isolated from fourteen BA patients and five CC patients human liver tissue using Mitochondrial Isolation Kit for Tissue (Thermo Scientific, Rockford, IL, USA). For the purpose, option A (Isolation of Mitochondria from Soft Tissues) from the manufacturer's protocol 1: Reagent-based Method for Soft Tissues was used. Briefly, each liver tissue (11 ~ 80 mg) were initially disrupted with 800 µL PBS in pre-chilled 2 mL glass dounce (Wheaton, Millville, NY, USA). Provided reagents and centrifugation steps allowed for purification of a mitochondrial pellet.

Mitochondrial DNA was extracted from the isolated mitochondrial samples by using the QIAamp DNA Mini Kit (Quiagen, Valencia, CA, USA) as per option 'Isolation of genomic DNA from bacterial cultures'. Further the Extracted mitochondrial DNA was quantified by Qubit 2.0 fluorometer with the Qubit dsDNA HS assay Kit (Life Technologies, Carlsbad, CA, USA). While the quality was checked by 1% agarose gel electrophoresis.

4. Sequencing library construction (Figure 1)

Two types of sequencing libraries were prepared. One was prepared by using total extracted mitochondrial DNA and the other library was made from PCR amplified fragments of mitochondrial DNA to avoid from the nuclear DNA contamination in subsequent making library. For the PCR amplified library, initially the entire mitochondrial DNA was amplified as four fragment by using validated primer set of mitochondrial origin co-amplification that prevents nuclear DNA sequences.[29] The primers for fragment 1 were 14898F (5'-tagccatgcactactcaccaga-3') and 1677R (5-' gtttagctcagagcggtcaagt-3'), fragment 2 were 1404F (5'-acttaagggtcgaaggtggatt-3') and 6739R (5'-gatatcatagctcagaccatacc-3'), fragment 3 were 6511F (5'-ctgctggcatcactatactacta-3') and 10648R (5'-ggcacaatattggctaagaggg-3'), fragment 4 were

10360F (5'-gtctggcctatgagtgactaca-3') and 15349R (5'-gtgcaagaataggaggtggagt-3'). The DNA amplification was performed in a thermo cycler (TGRADIENT, Biometra, UK) using the Prime STAR HS DNA polymerase (Takara Bio, Ohtsu, Japan). The PCR conditions were followed as initial denaturation for 2 min at 95°C, followed by 30 cycles of denaturation at 95°C for 20 s, annealing step at 57°C for 40 s, extension at 72°C for 5 min and final extension at 72°C for 5 min. The expected size of PCR products were confirmed by 1% agarose gel electrophoresis (Figure 1).

Further the PCR products were purified with AMPure kit (Beckman Coulter, Brea, CA, USA) and pooled in equimolar amounts to make fragment sequencing library. For the 200 bp libraries 30 ~ 300 ng mitochondrial DNA or entire amplified DNA was sheared by Bioruptor Sonication system (Diagenode, Denville, NJ, USA). The rest of steps in the library preparation were performed according to the Ion Plus Fragment Library Kit and Ion DNA Barcoding 1–16 Kit (Life Technologies, Gaithersburg, MD, USA). Following the sheared DNA end repair, adapter ligation, the library was size selected using a 2% E-Gel SizeSelect (Invitrogen, Carlsbad, CA, USA) instrument then followed by 8 cycles of final PCR amplification. The quantification and size distribution of each library was done through Bioanalyzer 2100 (Agilent Technologies, Agilent Technologies, Santa Clara, CA, USA).

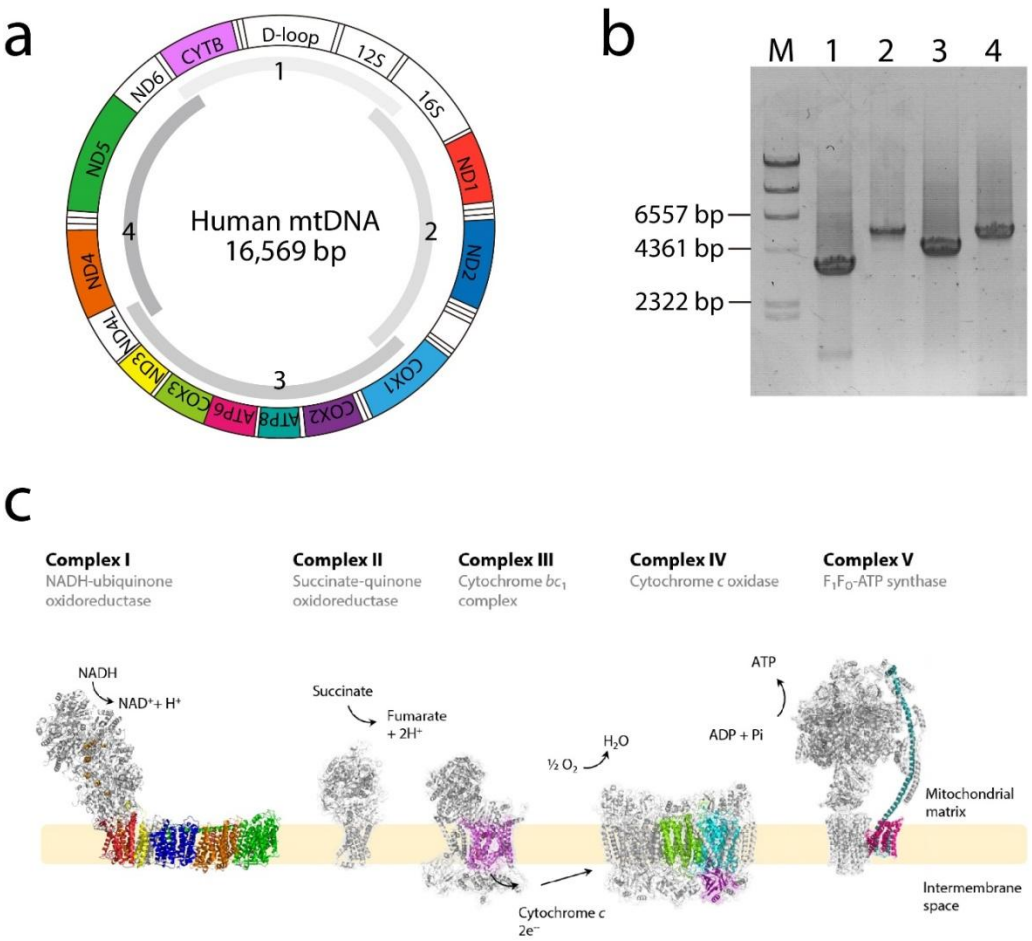

Figure 1. Schematic representation of the human mitochondrial genome and the respiratory chain in mitochondria. (a) Schematic representation of the 16,569 bp human mitochondrial genome with the protein-coding genes colored according to the complexes to which they contribute subunits, two ribosomal RNAs, 22 tRNAs and non-coding D-loop in white. Montage depicting the structural information currently available for the five complexes that together contribute to the mitocondrial oxidative phosphorylation machinery. (b) Electrophoresis of the amplified DNA fragments for mtDNA by PCR. M, *λ/HindIII* DNA marker; lane 1, PCR product 1 (3,580 bp); lane 2, PCR product 2 (5,548 bp); lane 3, PCR product 3 (4,447 bp); lane 1, PCR product 4 (5,591 bp). (c) The mammalian mitochondrial electron transport chain (ETC) includes the proton-pumping

enzymes complex I (NADH–ubiquinone oxidoreductase), complex III (cytochrome bc1) and complex IV (cytochrome c oxidase), which generate proton motive force that in turn drives F_1F_O-ATP synthase. Each complex is embedded in the lipid bilayer with the mitocondrial encoded subunits colored corresponding to the genome diagram. The structure of each respiratory complex is presented: complex I from *Thermus thermophilus* (protein databank (PDB) code 4HEA), complex II from porcine *Sus scrofa* (PDB 4YXD), complex III from bovine *Bos taurus* (PDB 1L0L), complex IV from bovine *B. taurus* (PDB 1OCC) and complex V from bovine *B. taurus* (PDB 5ARA).

5. Sequencing on a Ion Torrent Platform

For the clonal amplified sequencing templates, the libraries were pooled in equimolar amounts and emulsion PCR on Ion OneTouch system with Ion OneTouch 200 Template Kit v2 (Life Technologies, Gaithersburg, MD, USA). The templates were automatically enriched with the Ion OneTouch ES system (Life Technologies, Gaithersburg, MD, USA). Next Generation Sequencing (NGS) was performed using the Ion Torrent Personal Genome Machine (PGM) sequencer system using a 316D sequencing chip (Life Technologies, Gaithersburg, MD, USA).[30] Raw sequence data were analyzed by Ion Torrent Suite v4.0.2.

6. Sequence analysis of the mitochondrial genome

Homo sapiens mitochondrion, complete genome (revised Cambridge Reference Sequence, rCRS) was used as the reference sequence. FASTQ format sequence file was applied to sequence read mapping and variant calling by using Map Read to Reference tool and Quality-based Variant Detection tool in the CLC genomics workbench v7.0.3 software (CLC-bio, Aarhus, Denmark). Map Read to Reference with default parameters applying bioinformatic costs for mismatches of “2”, indel costs of “3”, length fraction of “0.5”, similarity fraction of “0.8” was performed. Quality-based Variant Detection with default parameters neighborhood radius of “5”, maximum gap and mismatch count of “2”, minimum neighborhood quality of “15”, minimum central quality of “20”, minimum coverage of “10”, minimum variant frequency (%) of “35”, variant filter of “Ion homopolymer indels” and genetic code “2 vertebrate mitochondrial”. The mitochondrial DNA haplogroups and mutations in encoding regions were determined by using MITOMAP[31] and MitoTool.[32]

III. Results

1. Histological and biochemical characteristics of patients (Table 1, 2)

The clinical characteristics of all patients having chronic liver diseases with BA and CC were examined as described in **Table 1**. In both groups of cholestatic patients, we found significant correlations in the age at the time of liver wedge biopsy during surgery and the parameters of hepatic injury and liver functions between two groups. The ages of BA patients at the time of liver wedge biopsy during surgery were younger than those of CC patients. In addition, their parameters of hepatic injury and liver function such as AST, ALT, AST to Platelet ratio index (APRI), D.Bil, *r*-GT, and prothrombine time-international normalized ratio (PT-INR) were higher than those of CC patients with P value < 0.05. However, both BA and CC groups did not show any significant difference in platelet count (PLT), protein, albumin, T.Bil, indicating that BA patients had relatively severe liver damage and hepatic dysfunction rather than CC patients. To investigate the state of those patients' livers in detail, we performed liver function tests (LFTs) for all 19 patients (**Table 2**). Consequently, all fourteen BA patients showed cholestasis with elevated levels of D.Bil and *r*-GT together with high levels of AST and ALT as parameters of hepatic injury. Based on the patients' clinical characteristrics, APRI, as an non-invasive serologic parameter of hepatic fibrosis, was significantly elevated in 9 BA patients (BA2, BA3, BA4, BA7, BA8, BA9, BA11, BA12, and BA14). In five CC patients, only AST level was elevated in four CC patients and most clinical characteristics including APRI were ranged at normal levels, indicating that CC patients showed relatively normal liver function and hepatic structure. However, such a liver injury was not correlated significantly with platelet count, protein, albumin, and T.Bil. Hepatic fibrosis in CC patients did not seem to be directly related to liver mitochondrial

dysfunction, whereas BA patients showed a severe hepatic damage with high levels of AST and ALT. Particularly, histological evaluation demonstrated that 9 BA patients (BA3, BA4, BA7, BA8, BA9, BA11, BA12, BA13, and BA14) exhibited severe destruction of normal hepatic structure (METAVIR ≥ 3) like hepatic fibrosis and cirrhosis. However, all CC patients presented no significant hepatic fibrosis with normal hepatic structure (METAVIR = 0). Based on these two METAVIR and APRI systems, it was ensured that significantly histological and clinical hepatic fibrosis could be seen in 8 BA patients (BA3, BA4, BA7, BA8, BA9, BA11, BA12, and BA14). Among these patients, values for albumin and PT-INR in 4 BA patients (BA4, BA7, BA9, and BA12) were significantly decreased rather than normal, indicating that their hepatic synthesis were dysfunctioned. However, the other BA patients (BA3, BA8, BA11, and BA14) appeared to retain hepatic biosyntheyic functions relatively higher than the former patients described above. Therefore, our histological and biochemical examination clearly indicated that both CC and BA patients showed liver injury. However, in the case of BA patients, the degree of liver function was differentially expressed in a patient-dependent manner.

Table 1. Comparison of clinical characteristics of all liver disease patients between BA and CC groups

	Total (N = 19)	BA (N = 14)	CC (N = 5)	*P*
Male (%)	8 (42.1)	7 (50.0)	1 (20.0)	
Age (weeks)	15.88 ± 16.80	19.18 ± 17.73	6.67 ± 10.21	0.033
AST (IU/L)	695.2 ± 2095.5	925.1 ± 2421.4	51.4 ± 21.9	0.002
ALT (IU/L)	295.7 ± 620.1	396.0 ± 700.9	15.0 ± 9.4	0.003
T.Bil (mg/dL)	8.07 ± 2.73	8.35 ± 1.82	7.28 ± 4.66	NS
D.Bil (mg/dL)	4.97 ± 3.06	6.50 ± 1.85	0.70 ± 0.35	0.001
Protein (g/dL)	5.75 ± 0.63	5.65 ± 0.70	5.60 ± 0.31	NS
Albumin (g/dL)	3.68 ± 0.49	3.66 ± 0.54	3.76 ± 0.36	NS
γ-GT (IU/L)	578.7 ± 779.7	733.4 ± 860.4	145.8 ± 109.0	0.006
Platelet	354.4 ± 124.4	353.6 ± 133.5	356.8 ± 108.3	NS
PT-INR	1.07 ± 0.31	1.10 ± 0.35	0.98 ± 0.06	0.002
APRI	13.213 ± 48.676	17.771 ± 56.529	0.454 ± 0.245	0.002
Metavir stage, 0/1/2/3/4	5/0/5/8/1	0/0/5/8/1	5/0/0/0/0	

All data show mean ± SD. AST = aspartate aminotrasferase; ALT = alanine aminotransferase; T.Bil = total bilirubin; D.Bil = direct bilirubin; γ-GT = gamma-glutamyl transpeptidase; PT-INR = prothrombine time-international normalized ratio.

Table 2. The histological and clinical characteristics of all patients

Patients	Sex	Age(wks)	Dx	METAVIR	AST	ALT	Platelet	APRI	T.Bil	D.Bil	Pro	Alb	*r*-GT	PT-INR
CC1	F	24.9	CC	0	66	31	309	0.628	0.3	0.2	6.0	4.3	24	1.05
CC2	M	2.9	CC	0	21	9	298	0.207	12.7	1.2	5.6	3.9	307	0.96
CC3	F	1.9	CC	0	48	12	331	0.427	9.5	0.7	5.3	3.7	73	0.9
CC4	F	1.9	CC	0	44	8	549	0.236	5.6	0.7	5.3	3.4	142	1.01
CC5	F	1.7	CC	0	78	15	297	0.772	8.3	0.7	5.8	3.5	183	0.97
BA1	M	14.9	BA	2	146	162	351	1.223	7.6	6.2	5.6	3.8	307	0.92
BA2	M	9.0	BA	2	202	98	275	2.160	11.1	9.1	5.4	3.4	382	0.94
BA3	M	15.4	BA	3	467	362	427	3.217	11.5	9.5	6.3	4.4	406	0.98
BA4	F	15.3	BA	3	330	244	505	1.922	9.6	7.5	5.2	3.1	644	1.34
BA5	F	3.9	BA	2	71	11	276	0.757	7.1	4	4.9	3.3	237	0.97
BA6	M	9.6	BA	2	174	114	379	1.350	6.1	4.9	5.4	3.8	422	0.98

BA7	F	10.1	BA	3	148	130	197	2.088	9	7.6	5.0	2.9	1145	1.19
BA8	M	61.0	BA	3	206	443	391	1.550	4.6	4	7.1	4.2	3371	1.03
BA9	M	11.3	BA	3	814	134	207	11.566	8.2	6.6	4.5	3.2	475	1.16
BA10	F	8.6	BA	2	155	179	545	0.837	8.3	6.7	5.6	4	246	0.99
BA11	F	17.9	BA	3	227	233	463	1.442	8.4	7.1	6.6	4.5	1658	0.85
BA12	F	58.7	BA	4	9310	2790	128	213.925	8.1	3.5	5.8	3	180	2.23
BA13	M	12.9	BA	3	184	193	542	0.999	7.6	6.4	6.2	4.2	541	0.81
BA14	F	19.9	BA	3	517	451	264	5.760	9.7	7.9	5.5	3.4	253	0.99

Age (wks) = Age at the time of liver wedge biopay (weeks); Dx = Diagnosis; AST = aspartate aminotrasferase (IU/L); ALT = alanine aminotransferase (IU/L); T.Bil = total bilirubin (mg/dL); D.Bil = direct bilirubin (mg/dL); Pro = Protein (g/dL); Alb = Albumin (g/dL); r-GT = gamma-glutamyl transpeptidase (IU/L); PT-INR = prothrombine time-international normalized ratio.

2. **Comparison of total DNA extract direct sequencing and mtDNA amplicon sequencing (Table 3-5 and Figure 1)**

To investigate whether the PCR-based amplicon sequencing can reflect the nucleotide variations in hepatic mtDNA from patients we examined in comparison with direct sequencing, we selectively chose three BA patients (BA7, BA12, and BA13) that exhibited clinical features differentially with respect to the extent of liver injury and liver function. As described in **Table 3**, for direct sequencing, we isolated mitochondria out of liver tissues and extracted mtDNAs, which were followed by the construction of mtDNA library. In case of mtDNA amplicon sequencing, total mtDNA extracts were amplified by PCR using four pairs of overlapping primers, yielding 3,580 bp, 5,548 bp, 4,447 bp, and 5,591 bp DNA fragments, respectively (**Figure 1a**). The amplified PCR products were used to prepare the mtDNA amplicon library. To discriminate the sequence data of individual patients, we linked an Ion Xpress Barcode Adapter sequence to each fragment in the direct sequencing and amplicon mtDNA libraries. Both mtDNA libraries were then subjected to sequencing with the Ion Torrent Personal Genome Machine (PGM) sequencer system. As described in **Table 3**, the direct sequencing results showed a relatively low coverage (< 50×) with the mapped mtDNA read percentage of less than 1% mainly due to the cross-contamination with nuclear DNA (ncDNA). On the other hand, despite the smaller total read counts than those of direct sequencing, mtDNA amplicon sequencing exhibited a high coverage (> 2,000×) with the mapped mtDNA read percentage of over 92%. Nevertheless, such huge different metrics generated by both sequencing approaches did not give any discrepant and biased results between them, indicating that mtDNA amplicon sequencing could provide high levels of identical results with respect to the total single nucleotide variation (SNV) row count when compared to direct sequencing. Indeed, we found the same SNV row count number and location for

BA7 patient from the direct and mtDNA amplicon sequencing results. Remarkably, mtDNA amplicon sequencing could find a 14766C>T variation in Patient 46 and 16183A>C, 16189T>C variations in Patient 49, which were not detected by direct sequencing because of insufficient mapped reads ascribed to its low average coverage (< 40×) (**Table 4 and 5**). Therefore, these results indicate that mtDNA amplicon library sequencing is an efficient approach to verify the mtDNA sequences of liver tissues over direct sequencing.

Table 3. SNVs in total DNA direct sequencing and mtDNA Amplicon sequencing

Sample: BA7

Position	Type	Reference	Allele	Direct sequencing			Amplicon sequencing		
				Count	Coverage	Frequency	Count	Coverage	Frequency
73	SNV	A	G	48	48	100	9570	9593	99.76
188	SNV	A	G	43	43	100	9295	9361	99.29
235	SNV	A	G	38	38	100	6893	6915	99.68
263	SNV	A	G	31	31	100	5688	5699	99.81
523	Deletion	A	0	16	18	88.89	2072	2436	85.06
663	SNV	A	G	32	33	96.97	8317	8348	99.63
750	SNV	A	G	37	38	97.37	10132	10336	98.03
1438	SNV	A	G	60	60	100	7681	7698	99.78
1736	SNV	A	G	29	29	100	20	20	100
2706	SNV	A	G	39	39	100	41	41	100
3107	Deletion	N	0	49	51	96.08	54	54	100
4248	SNV	T	C	8	13	61.54	13	17	76.47

4655	SNV	G	A	47	47	100	23	23	100
4769	SNV	A	G	52	54	96.3	29	29	100
4824	SNV	A	G	50	51	98.04	27	29	93.1
6915	SNV	G	A	46	46	100	94	94	100
7028	SNV	C	T	66	66	100	148	148	100
8563	SNV	A	G	37	40	92.5	35	35	100
8794	SNV	C	T	43	44	97.73	86	86	100
8860	SNV	A	G	48	49	97.96	86	86	100
11536	SNV	C	T	34	34	100	309	338	91.42
11647	SNV	C	T	28	38	73.68	359	364	98.63
11719	SNV	G	A	42	42	100	332	338	98.22
12705	SNV	C	T	40	53	75.47	413	550	75.09
14757	SNV	T	C	17	19	89.47	123	128	96.09
14766	SNV	C	T	20	22	90.91	110	114	96.49
15326	SNV	A	G	28	28	100	4686	4734	98.99
16187	SNV	C	T	48	48	100	3886	3973	97.81

16209	SNV	T	C	51	51	100	4271	4282	99.74
16223	SNV	C	T	41	42	97.62	3195	3649	87.56
16290	SNV	C	T	29	29	100	4021	4048	99.33
16319	SNV	G	A	22	22	100	3443	4738	72.67

Sample: BA12

Position	Type	Reference	Allele	Direct sequencing			Amplicon sequencing		
				Count	Coverage	Frequency	Count	Coverage	Frequency
73	SNV	A	G	15	15	100	9859	9881	99.78
235	SNV	A	G	13	13	100	7308	7342	99.54
263	SNV	A	G	10	10	100	6160	6180	99.68
663	SNV	A	G	20	20	100	8314	8357	99.49
750	SNV	A	G	25	25	100	10037	10251	97.91
1438	SNV	A	G	32	34	94.12	8361	8376	99.82
1736	SNV	A	G	13	13	100	54	56	96.43
2706	SNV	A	G	25	25	100	121	121	100

3107	Deletion	N	0	28	28	100	150	150	100
4248	SNV	T	C	9	13	69.23	34	41	82.93
4655	SNV	G	A	22	23	95.65	72	74	97.3
4736	SNV	T	C	29	29	100	89	90	98.89
4769	SNV	A	G	27	29	93.1	97	98	98.98
4824	SNV	A	G	19	24	79.17	98	100	98
5773	SNV	G	A	25	25	100	84	84	100
7028	SNV	C	T	34	34	100	1107	1109	99.82
8563	SNV	A	G	13	20	65	259	264	98.11
8794	SNV	C	T	21	21	100	596	599	99.5
8860	SNV	A	G	19	19	100	613	616	99.51
10801	SNV	G	A	23	24	95.83	1981	2003	98.9
11536	SNV	C	T	17	17	100	1307	1427	91.59
11647	SNV	C	T	23	27	85.19	1468	1480	99.19
11719	SNV	G	A	27	29	93.1	1422	1428	99.58
12705	SNV	C	T	15	18	83.33	1565	2013	77.74

12880	SNV	T	C	25	25	100	2092	2098	99.71
14766	SNV	C	T				420	439	95.67
14944	SNV	C	T	19	19	100	11093	11207	98.98
15326	SNV	A	G	24	24	100	5398	5436	99.3
16187	SNV	C	T	13	14	92.86	3861	3978	97.06
16223	SNV	C	T	10	13	76.92	2894	3425	84.5
16290	SNV	C	T	10	10	100	3977	4019	98.95
16319	SNV	G	A	10	11	90.91	3340	4566	73.15

Sample: BA13

Position	Type	Reference	Allele	Direct sequencing			Amplicon sequencing		
				Count	Coverage	Frequency	Count	Coverage	Frequency
73	SNV	A	G	19	19	100	4721	4734	99.73
263	SNV	A	G	18	18	100	2970	2974	99.87
709	SNV	G	A	18	18	100	4285	4355	98.39
750	SNV	A	G	18	18	100	4689	4788	97.93

1119	SNV	T	C	28	28	100	3616	3633	99.53
1438	SNV	A	G	24	24	100	5283	5292	99.83
2706	SNV	A	G	31	31	100	748	751	99.6
3107	Deletion	N	0	27	28	96.43	904	909	99.45
3497	SNV	C	T	19	20	95	288	294	97.96
4769	SNV	A	G	30	31	96.77	652	661	98.64
7028	SNV	C	T	36	36	100	1816	1831	99.18
7772	SNV	A	G	34	34	100	1293	1328	97.36
8860	SNV	A	G	17	17	100	1110	1110	100
10310	SNV	G	A	39	39	100	1078	1085	99.35
11719	SNV	G	A	31	31	100	1697	1706	99.47
14133	SNV	A	G	17	17	100	886	891	99.44
14766	SNV	C	T	12	12	100	447	461	96.96
15326	SNV	A	G	35	35	100	3726	3754	99.25
15346	SNV	G	A	34	34	100	2435	4010	60.72
15924	SNV	A	G	29	30	96.67	4260	4264	99.91

16086	SNV	T	C	27	27	100	3811	3840	99.24
16183	SNV	A	C				262	431	60.79
16189	SNV	T	C				784	921	85.12
16217	SNV	T	C	12	12	100	1463	1481	98.78
16311	SNV	T	C	17	17	100	2412	2414	99.92
16519	Deletion	T	0	14	21	66.67	3889	4108	94.67

Table 4. Sequencing metrics of total DNA extract and mtDNA amplicon

Sample	BA7		BA12		BA13	
	Total DNA extract	mtDNA Amplicon	Total DNA extract	mtDNA Amplicon	Total DNA extract	mtDNA Amplicon
Total reference length (bp)	16,569	16,569	16,569	16,569	16,569	16,569
Total read count	521,196	226,135	499,861	314,756	511,511	251,829
Mapped mtDNA read count	4,899	210,745	2,482	293,863	3,093	232,972
Mapped read percentage (%)	0.94	93.19	0.50	99.36	0.60	92.51
Average coverage	42×	2,034×	22×	2,705×	26×	2,164×
SNV row count	32	32	31	32	24	26

Runs of all three patients‘ samples were performed independently in triplicates.

Table 5. Pattern analysis of mitochondrial DNA

Patients	Diagnosis	Haplogroup	SNV row count	Total read count	Mapped mtDNA read count	Average Coverage
CC1	CC	D4a	41	264,985	244,915	2,389×
CC2	CC	N9a8	26	121,290	118,291	1,739×
CC3	CC	N9a3	27	249,601	240,810	4,028×
CC4	CC	G2a1d1a	46	355,254	345,667	5,119×
CC5	CC	D4e2	36	425,521	410,639	6,535×
BA1	BA	D5b1a	41	162,707	150,677	1,490×
BA2	BA	D5a2a1a	41	302,545	278,928	2,777×
BA3	BA	D4h1a1	42	146,728	141,966	2,052×
BA4	BA	A5a1a1b	34	152,570	148,301	2,330×
BA5	BA	D4	36	101,832	99,088	1,578×
BA6	BA	B4a2b	31	248,273	230,326	2,264×
BA7	BA	A5a	33	226,135	210,745	2,108×
BA8	BA	D4	40	203,118	197,954	2,971×
BA9	BA	A11	30	99,617	97,557	1,596×
BA10	BA	M8a3a1	39	76,196	73,945	1,119×
BA11	BA	B4c1a1	29	577,938	564,294	8,472×
BA12	BA	A5a1a1b	34	314,756	293,863	2,807×
BA13	BA	B4c1a1a	27	251,829	232,972	2,250×
BA14	BA	D5b	45	454,096	441,527	7,318×
Total	-	-	678	4,734,991	4,522,465	-

3. Molecular genetic analysis for patients (Table 5, 6 and Figure 2, 3)

To rapidly detect SNVs, mtDNA amplicon libraries derived from mtDNAs for 19 patients were constructed. Upon completion of the analysis, we obtained a total of 4,734,991 raw reads for all 19 samples with an average coverage of > 1,000× (**Table 5**). From 19 sets of mtDNA sequences, 678 SNVs were identified. Out of these SNVs, 151 non-synonymous variations were found in the 13 mitochondrial protein coding sequences in **Table 6** and **Figure 2.** The CYB region had the highest number of non-synonymous SNVs (41 SNVs), followed by 39 SNVs in ATP6, 17 SNVs in DN4, 16 SNVs om ND2, 10 SNVs in ND3, 7 SNVs in CO2, 6 SNVs in ATP8, 6 SNVs in ND1, 5 SNVs in ND5, 3 SNVs in CO1, and one SNV in CO3, respectivly (**Figure 3**). However, SNVs were not identified in ND4L and ND6. Remarkably, novel SNVs were identified in CO2 (L179stop) in six samples (BA1, BA2, BA6, BA7, BA12, and BA13), ATP8 (M42stop) in one sample (CC1), and ND4 (S97stop) in eight samples (CC1, CC5, BA3, BA8, BA9, BA10, BA11, and BA14) in the study. Novel SNVs had relatively low frequency (35.64 ~ 69.32%) when compared with others. All samples, showed haplogroup originated in Asia except the reference (http://www.ncbi.nlm.nih.gov/nuccore/251831106).

Table 6. Non-synonymous variations in mitochondrial DNA encoding regions

Patient	Locus										
	ND1	ND2	CO1	CO2	ATP8	ATP6	CO3	ND3	ND4	ND5	CYB
CC1		L237M			L17F M42stop	T59A T112A		T114A	Y95H S97stop		T7II78T T194A
CC2						T112A				T8A	T7I I115T T194A
CC3	T275A					T112A				T8A	T7I T194A
CC4		T122A				T59A T112A		T114A			T7I T194A
CC5		L237M	V128I		L17F	T59A T112A		T114A	Y95H S97stop		T7I T194A
BA1		L237M I278V	M117T	L179stop		T59A T112A		T114A			T7I T194A

BA2		L237M I278V		L179stop		T59A T112A	T114A	I423V	T7I T194A
BA3	V113A	L237M			L17F	T59A T112A	T114A	Y95H S97stop	T7I T194A
BA4		T119A				T13A H90Y T112A		F182L	T7I T194A
BA5		L237M			L17F	T59A T112A	T114A	T449A	T7I T194A
BA6				L179stop		T112A V142I			T7I T194A
BA7		T119A	V338M	L179stop		T13A H90Y T112A			M4T T7I T194A
BA8	T153M	L237M			L17F	T59A T112A	T114A	Y95H S97stop	T7I T194A

BA9		T119A		H90Y T112A			Y95H S97stop	T7I T194A
BA10				A20T T59A T112A		T114A	Y95H S97stop	T7I T194A
BA11	Y43C A64V			T112A			Y95H S97stop	T7I T194A
BA12		T119A	L179stop	T13A H90Y T112A			F182L	T7I
BA13	A64V		T63A L179stop	T112A				T7I T194A
BA14		L237M I278V		T59A T112A A207T	V248I	T114A	Y95H S97stop	T7I T194A

Runs of all 19 patients‘ samples were performed independently in triplicates.

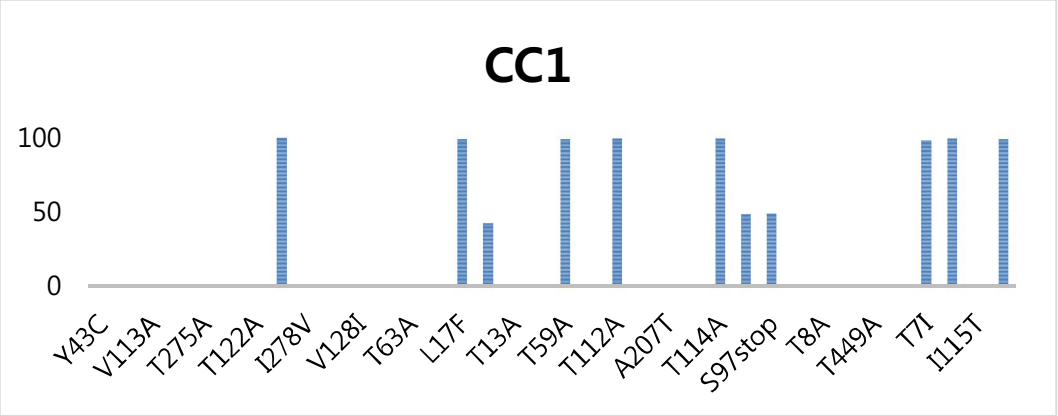

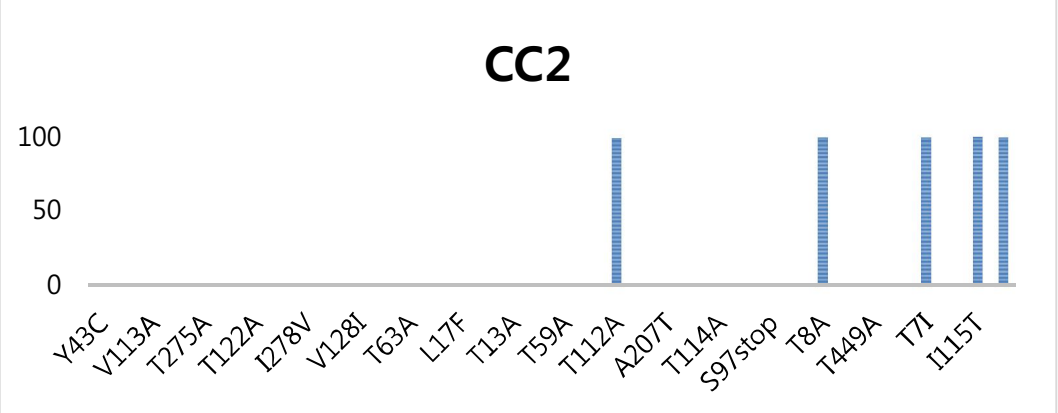

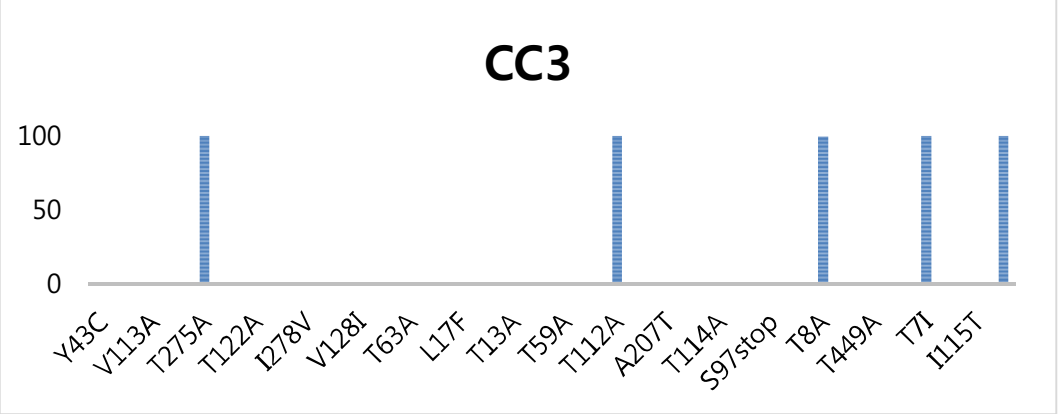

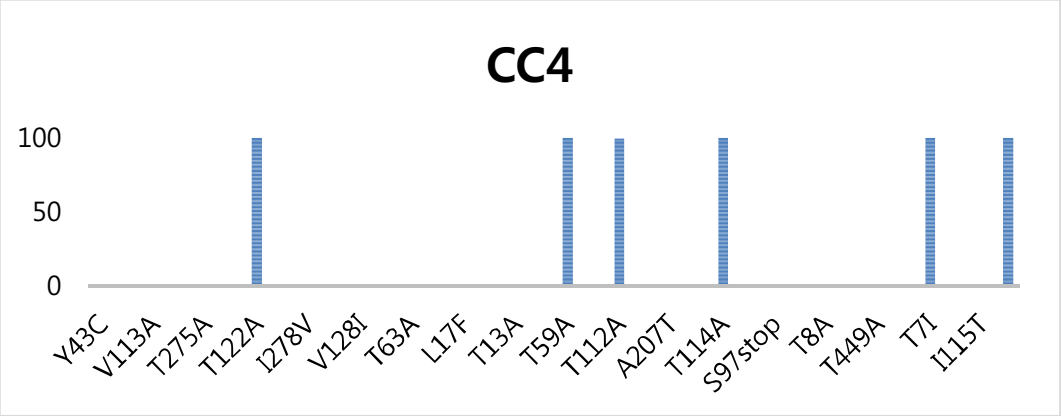

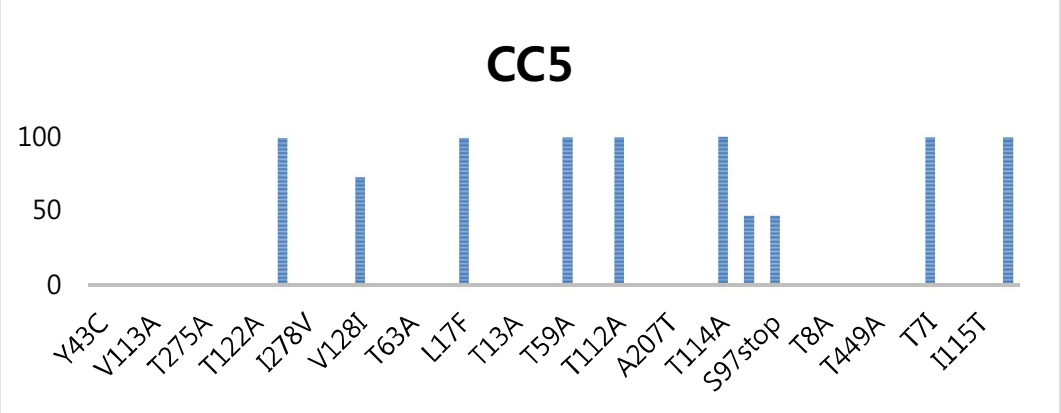

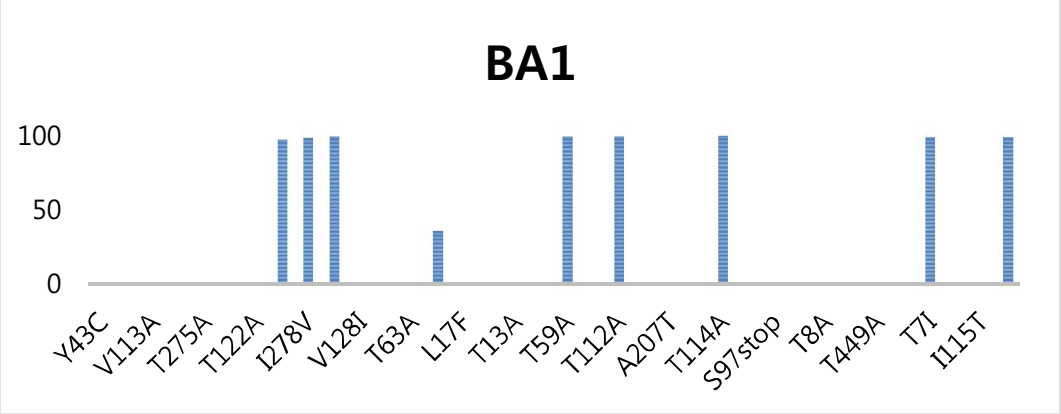

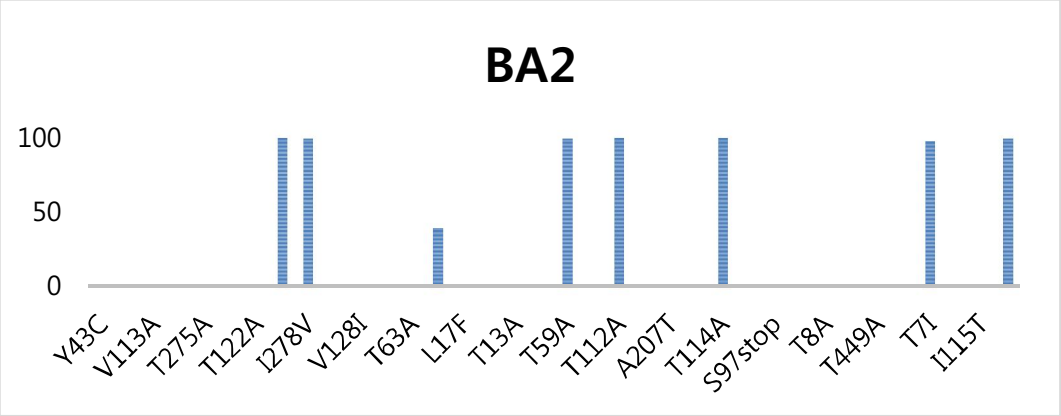

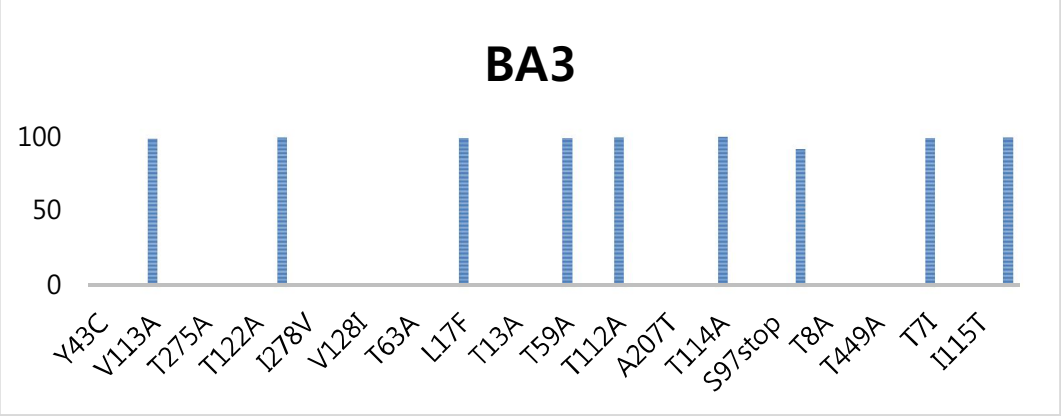

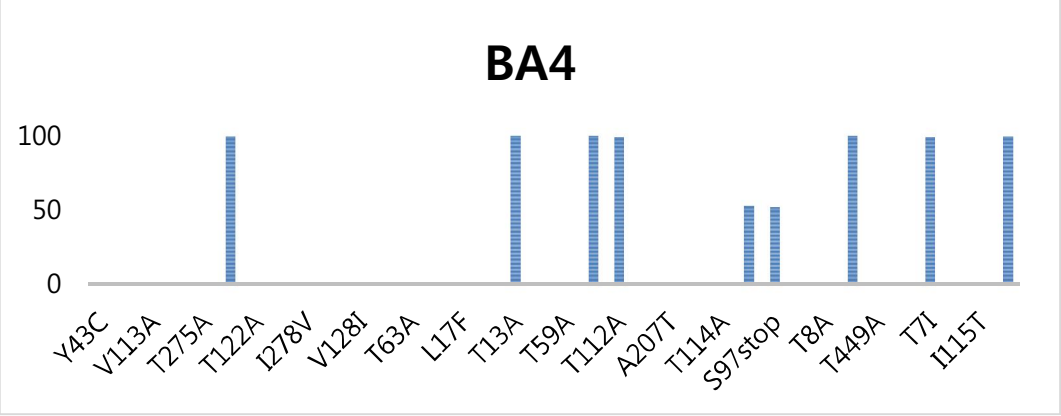

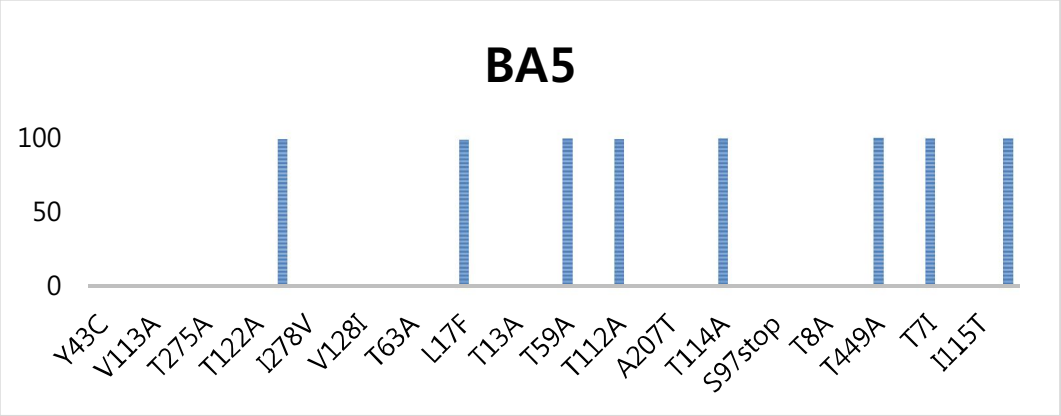

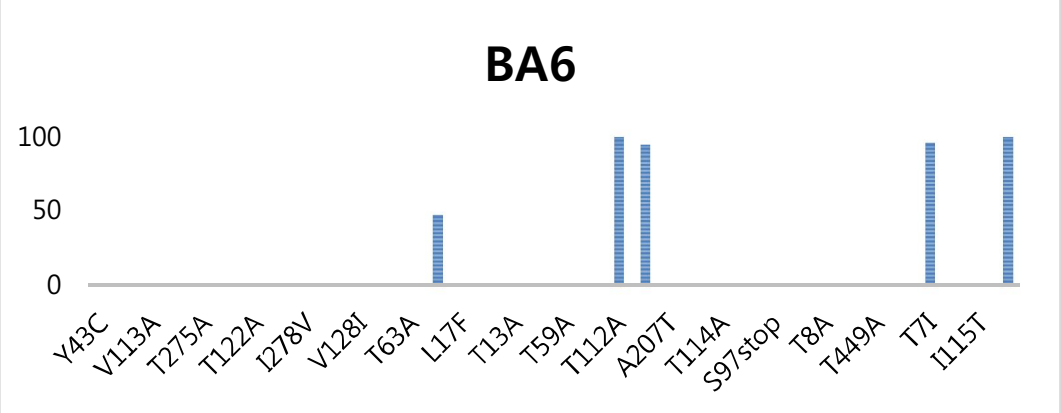

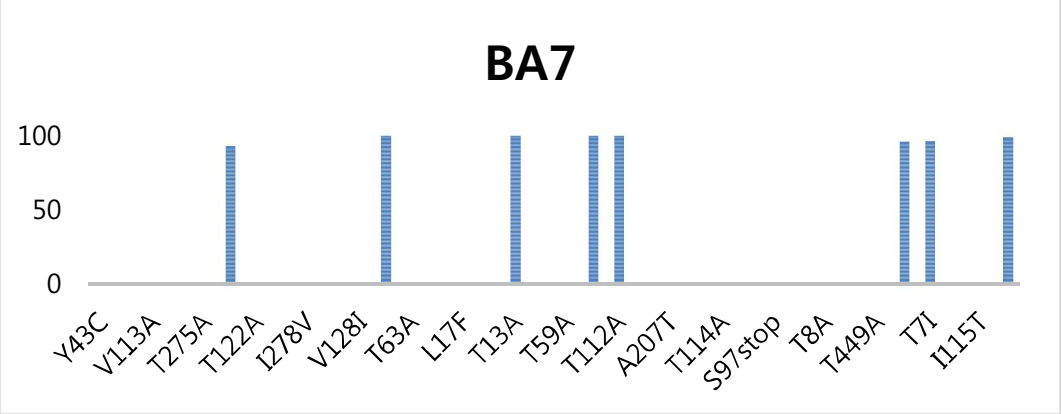

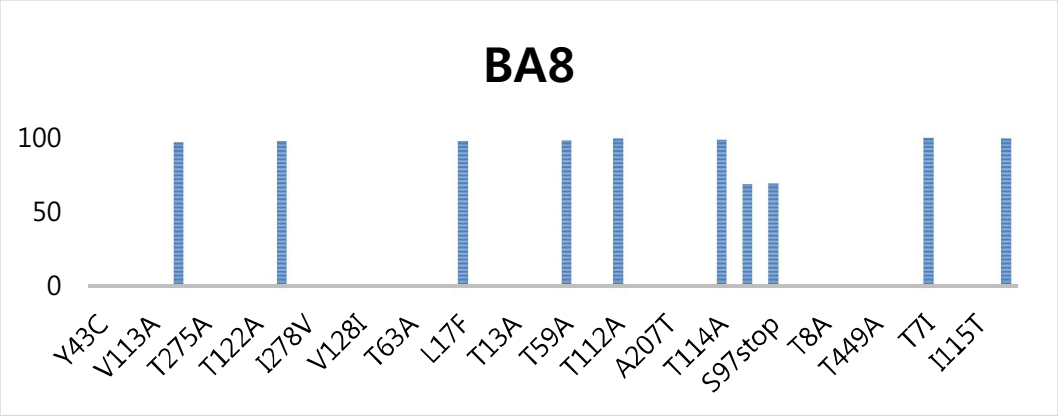

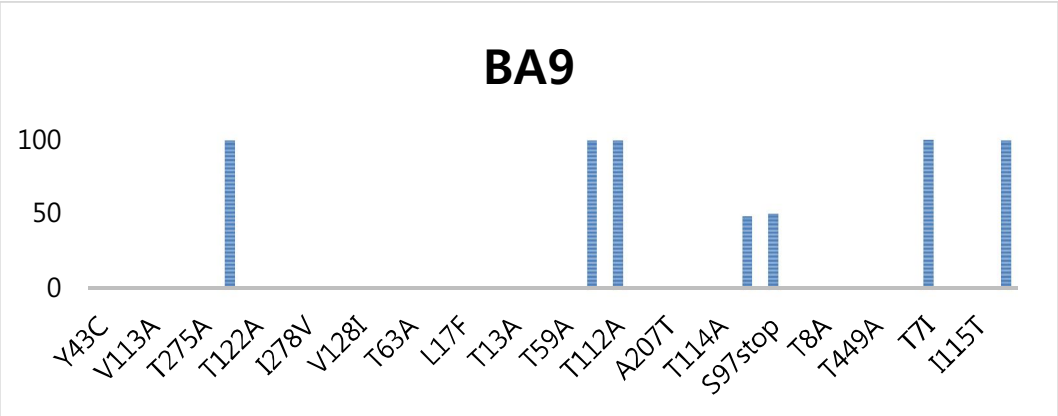

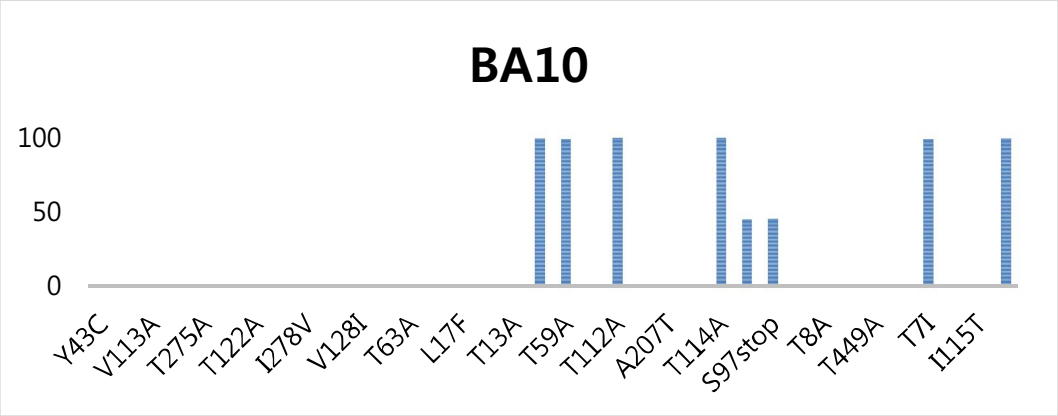

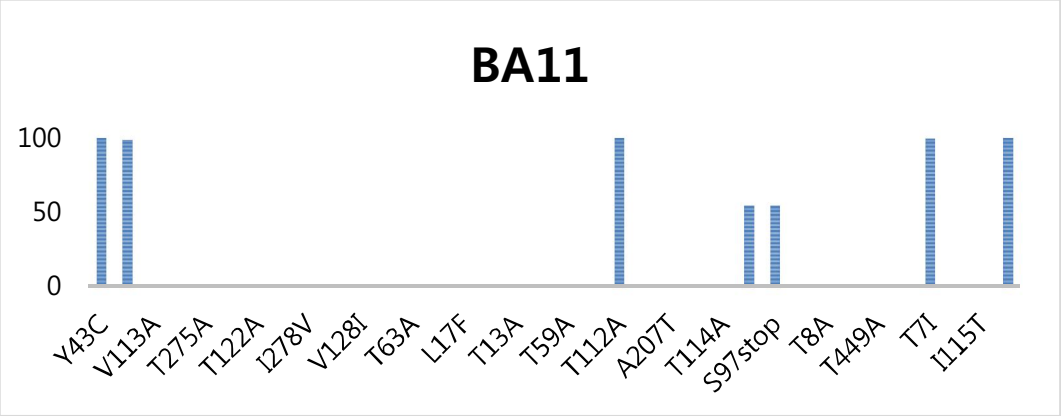

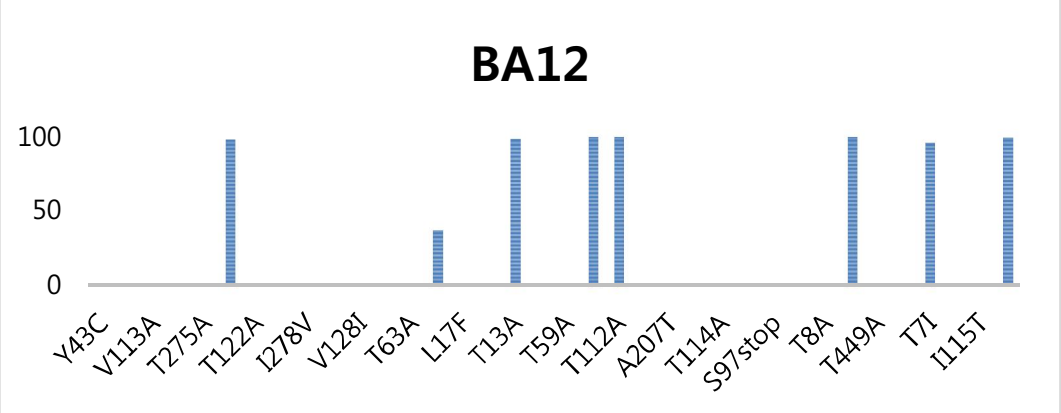

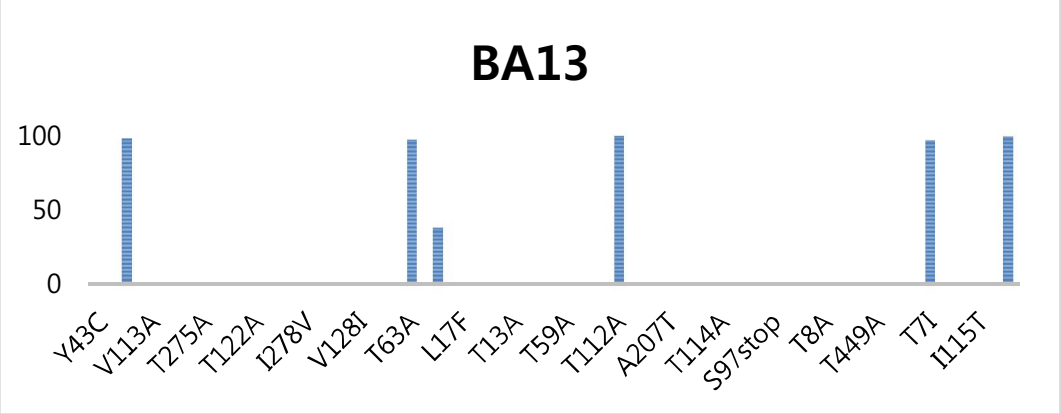

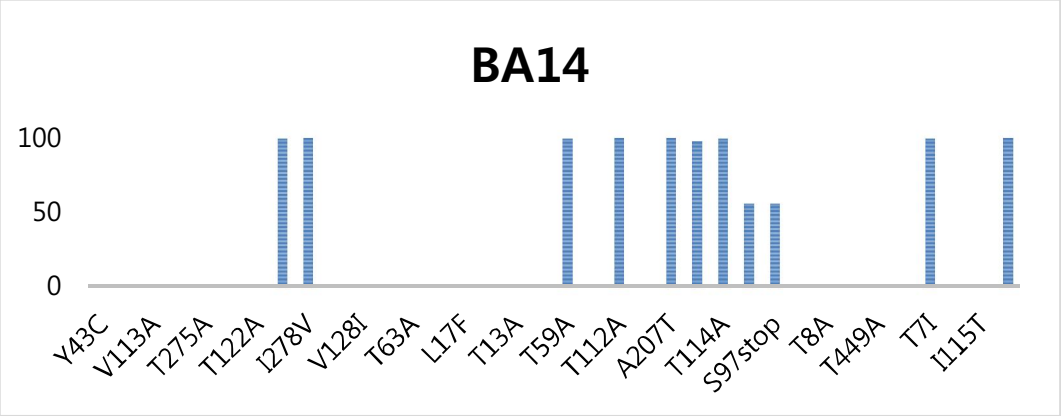

Figure 2. The relative frequency of non-synonymous variations in mtDNAs encoding the respiratory chains in all patients.

a

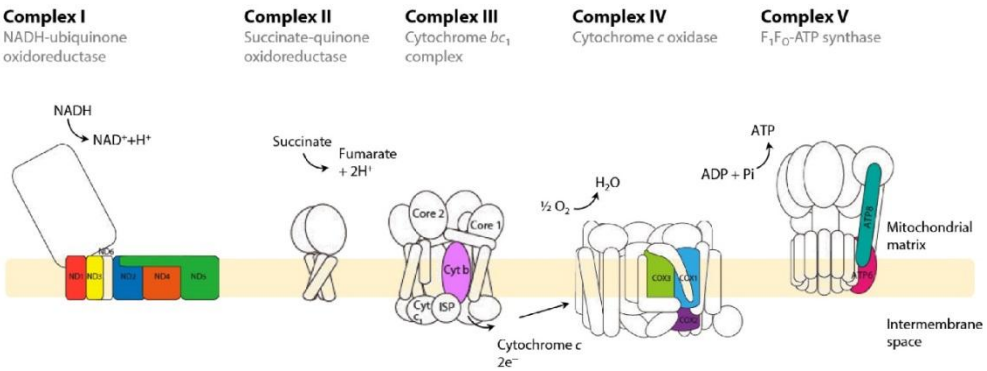

Y43C T114A T119A Y95H T8A
A64V T122A S97Stop F182L
V113A I278V I423V T449A
T153M L237M
T275A

T7I
I78T
I115T
T194A

V248I M117T T63A
V128I
V338M

T13A L17F
A20T
T59A
H90Y
T112A
V142I
A207T

b

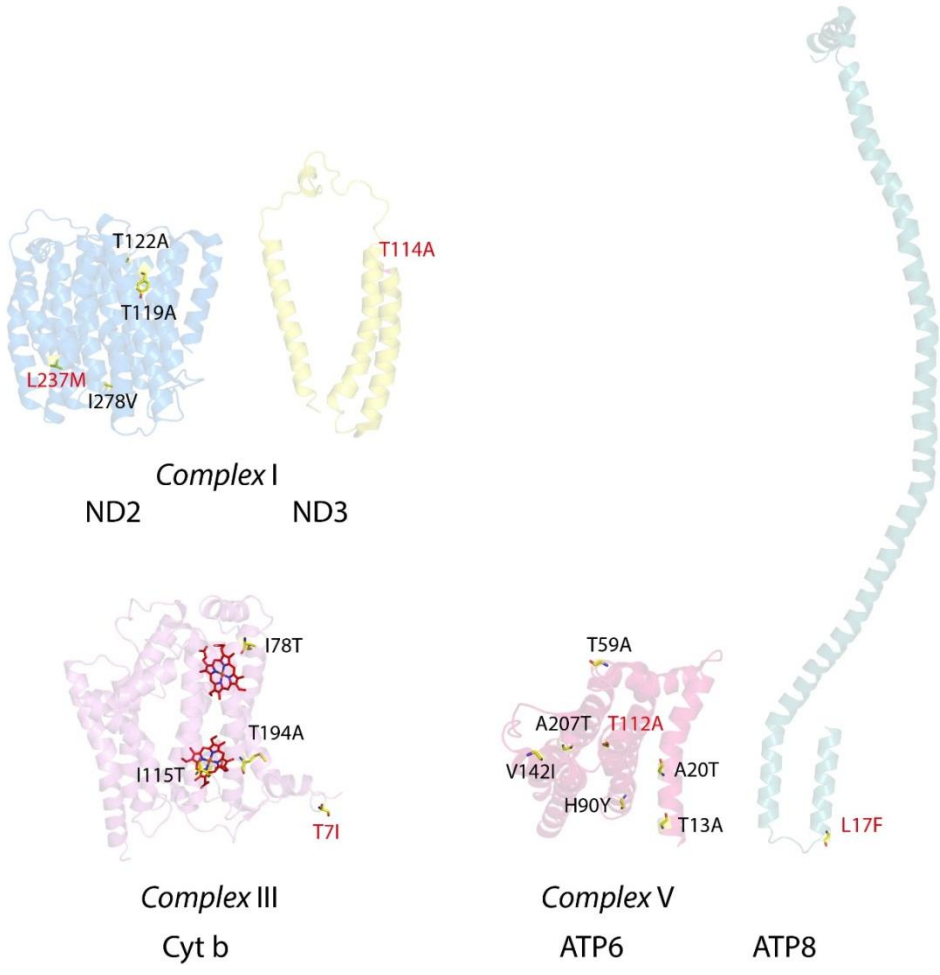

Figure 3. (a) Schematic presentation of the magnified view of the intermembrane space and mitochondrial membrane with complexes of the electron transport chain. (b) Location of missense mutations on the mitochondria complex. Close up views of the ND2 and ND3 of complex I, Cyt b of complex III, or ATP and ATP8 of complex V. The sites of the mutations are indicated in sticks and yellow.

IV. DISCUSSION

Recent studies reveal that mutations in protein-coding mtDNA genes in liver have been associated with hepatocellular dysfunction.[33] Particularly, chronic liver diseases by BA, which is an important cause of liver failure at infancy, undergo progressive hepatological deterioration. Even after Kasai surgery, this developmental failure by BA often does not guarantee a positive prognosis, frequently resulting in chronic liver failure.[34] As BA progresses, symptoms may also include episodes of bile acidosis and lack of hepatic biosynthesis, which may lead to impairment of respiratory and liver function involved in hepatic functionality. Most chronic liver diseases have defects of mitochondrial energy production, such as deficiency of an enzyme of the mitochondrial respiratory chain complex.[14] Very recently, Zeharia and coworkers reported that two patients suffered from a lethal neurodegenerative disorder of infantile onset accompanied by hepatocellular dysfunction.[35] Based on increased plasma lactate and alanine levels, and abnormal urinary organic acid profile with 3-methylglutaconic aciduria and excessive excretion of Krebs cycle metabolites, mitochondrial respiratory chain defect seemed to be a suspected cause, which was supported by decreased activities in the mitochondrial respiratory chain complexes I, III and IV in the patients' livers using exome analysis. In addition, an established mouse model demonstrated the distinct metabolic alterations in mice with a mitochondrial polymorphism associated hepatic mitochondrial dysfunction linked to a non-synonymous gene variation (nt7778 G/T) of ATP8.[36]

BA hepatic encephalopathy appears usually due to mutations in one or more of the eleven genes encoding subunits of complexes I, III, IV, and V. In both CC and BA patients, three mutations in mtDNA were found dominantly in ATPase 6 of complex V (i.e., T112A) and cytochrome *b* of complex III (T7I, and T194A), suggesting that these

mutations are highly associated with liver dysfunction. Additional frequent mutations (L237M, T114A, and L17F) were also found in ND2 and ND3 of complex I and ATP8 of complex V, respectively. All nineteen patients had hepatitis that began at infancy and became progressively worse. For reasons that are not clear, mitochondrial proliferation is not prominent in these two patient groups. Consequently, NGS-based genomic studies showed that mutations in complex I in twelve BA patients, whereas all fourteen BA patients exhibit the genetic heterogeneity of this condition. Notably, four (BA4, BA7, BA9, and BA12) of fourteen BA patients described here were found to have distinct pathogenic mutations (T119A and I278V) in still another mtDNA protein-coding gene, that for ND2. Indeed, hepatic dysfunction as well as liver impairment was severely present in all four patients. Another set of mutations in ND4 of complex I (i.e., Y95H and S97stop) were found in four (BA3, BA8, BA11, and BA14) of BA patients. Those patients' livers were severely fibrotic damaged, whereas there was no other hepatological functional abnormality. Liver biopsy showed multifocal spotty necrosis, cholestasis, portal and lobular lymphocytic infiltration with cirrhosis in BA patients. The mutations were considered pathogenic on the basis of several findings. First, all were heteroplasmic, which is associated with deleterious mutations rather than neutral polymorphisms. Y95H and S97stop were non-synonymous mutations, resulting in truncated ND4 molecules. The other two mutations (T119A and I278V) for ND2 were substitutions of highly conserved nucleotides. In all BA patients having the former mutations described above the clinical and biochemical characteristics on their liver functions showed a strong correlation between pathologic changes (cirrhosis) and the frequency of mutant mtDNA. Mutations in the ND4 protein are very critical for Leber Hereditary Optic Neuropathy due to a disorder with oxidative phosphorylation deficiency.[37] Recent studies suggest that mutated ND2 protein impairs mitochondrial complex I assembly, which leads to Leigh syndrome

and proton pumping activity.[38,39] Both ND4 and ND2 subunits of complex I are located in proximity to be associated with the other subunit in mitochondrial membranes, and ND2 must be functional for proton transfer to occur. All the non-synonymous mutations are located within or close to the contact region between intersubunits and are likely to prevent assembly and proton pumping pathway, with loss of enzyme activity (**Figure 3**). In this aspect, we strongly believed that these mutations found in BA patients are obviously pathogenic, but functional assay has not been verified in cultured cells expressing these genetic mutations. The high frequency of somatic mutations in the cytochrome b and ATPase 6 genes may seem surprising but is in keeping with the large number of polymorphisms observed in the same gene in CC patients. Moreover, the fact that all pathogenic mutations identified in our BA patients consisted of the substitution of adenine for guanine, further speculates that they may result from oxidative damage. At this stage, we cannot conclude that the mutations in the ND2 and ND4 genes of complex I in our BA patients are likely to have been somatic. The finding of hepatic failure in a patient with BA and no family history of hepatic disorder should alert the clinician to the possibility of either ND2 or ND4 gene mutation. Confirmation of the diagnosis requires liver biopsy to investigate complex I deficiency and to identify the molecular defect.

BA is still the most common cause of liver transplantation in children even after successful Kasai operation and cholestasis after surgery can lead the liver to the end-stage liver disease occurring mitochondrial damage in hepatocyte. Until now, the pathophysiology was still unknown. The further study to identify the exact mechanism of hepatic mitochondrial damage in chronic liver disease is highly required to understand the progression to the end-stage liver disease. In this study, mtDNA analysis with BA patients using an NGS-based amplicon library sequencing revealed that all mtDNA samples derived from 15 mg liver tissues were sequenced deeply enough for accurate SNV

detection with average coverage of over 1000× and the mapped read percent of over 92%. Thus, we strongly believe that the amplicon sequencing enables us to identify SNPs in hepatic mtDNAs, which can be a promising approach to establish the mitochondrial pathophysiology and biochemical mechanism of hepatic dysfunction in chronic liver disease.

V. CONCLUSION

This is the first study to investigate the extent of mtDNA mutaion in the liver of BA patients using a next-generation sequencing technique, particularly focusing on the genes encodeing energy transducing components involved in the respiratory chain, together with those of livers from CC patients as a counterpart and highlights the role of mitochondrial function in normal cell physiology and BA disease to elucidate pathological mechanism associated with mitochondrial dysfunctions.

However, there are some limitations in this study: (1) a small mumber of patients were studied, (2) impaired mitochondrial functions were not assessed using mitochondrial function assay technique. Nevertheless, this study suggests that the amplicon sequencing enables us to identify SNPs in hepatic mtDNAs, which can be a promising approach to establish the mitochondrial pathophysiology and biochemical mechanism of hepatic dysfunction in chronic liver disease.

REFERENCES

1. Trauner M, Meier PJ, Boyer JL. Molecular pathogenesis of cholestasis. N Engl J Med 1998;339:1217-27.
2. Bezerra JA. The next challenge in pediatric cholestasis: deciphering the pathogenesis of biliary atresia. J Pediatr Gastroenterol Nutr 2006;43 Suppl 1:S23-9.
3. Reyes H. Review: intrahepatic cholestasis. A puzzling disorder of pregnancy. J Gastroenterol Hepatol 1997;12:211-6.
4. Thompson RJ, Azevedo RA, Galoppo C, Lewindon P, McKiernan P, European Society for Paediatric Gastroenterolgo, Hepatology and Nutrition. Cholestatic and metabolic liver diseases: Working Group report of the second World Congress of Pediatric Gastroenterology, Hepatology, and Nutrition. J Pediatr Gastroenterol Nutr 2004;39 Supple 2:S611-5.
5. Alpini G, Glaser SS, Ueno Y, Rodgers R, Phinizy JL, Francis H, et al. Bile acid feeding induces cholangiocyte proliferation and secretion: evidence for bile acid-regulated ductal secretion. Gastroenterology 1999;116:179-86.
6. Heathcote EJ. Diagnosis and management of cholestatic liver disease. Clin Gastroenterol Hepatol 2007;5:776-82.
7. Li MK, Crawford JM. The pathology of cholestasis. Semin Liver Dis 2004;24:21-42.
8. Malhi H, Gores GJ. Cellular and molecular mechanisms of liver injury. Gastroenterology 2008;134:1641-54.
9. Chinnery PF, DiMauro S. Mitochondrial hepatopathies. J Hepatol 2005;43:207-9.
10. Johns DR. Seminars in medicine of the Beth Israel Hospital, Boston. Mitochondrial DNA and disease. N Engl J Med 1995;333:638-44.

11. Morris AA, Taanman JW, Blake J, Cooper JM, Lake BD, Malone M, et al. Liver failure associated with mitochondrial DNA depletion. J Hepatol 1998;28:556-63.
12. Sokol RJ, Treem WR. Mitochondria and childhood liver diseases. J Pediatr Gastroenterol Nutr 1999;28:4-16.
13. Fromenty B, Pessayre D. Inhibition of mitochondrial beta-oxidation as a mechanism of hepatotoxicity. Pharmacol Ther 1995;67:101-54.
14. Grattagliano I, Russmann S, Diogo C, Bonfrate L, Oliveira PJ, Wang DQ, et al. Mitochondria in chronic liver disease. Curr Drug Targets 2011;12:879-93.
15. Malhi H, Guicciardi ME, Gores GJ. Hepatocyte death: a clear and present danger. Physiol Rev 2010;90:1165-94.
16. Krahenbuhl L, Talos C, Reichen J, Krahenbuhl S. Progressive decrease in tissue glycogen content in rats with long-term cholestasis. Hepatology 1996;24:902-7.
17. Lang C, Berardi S, Schafer M, Serra D, Hegardt FG, Krahenbuhl L, et al. Impaired ketogenesis is a major mechanism for disturbed hepatic fatty acid metabolism in rats with long-term cholestasis and after relief of biliary obstruction. J Hepatol 2002;37:564-71.
18. Lang C, Schafer M, Serra D, Hegardt F, Krahenbuhl L, Krahenbuhl S. Impaired hepatic fatty acid oxidation in rats with short-term cholestasis: characterization and mechanism. J Lipid Res 2001;42:22-30.
19. Bogenhagen DF. Repair of mtDNA in vertebrates. Am J Hum Genet 1999;64:1276-81.
20. Bohr VA, Anson RM. Mitochondrial DNA repair pathways. J Bioenerg Biomembr 1999;31:391-8.
21. Mansouri A, Gaou I, De Kerguenec C, Amsellem S, Haouzi D, Berson A, et al. An alcoholic binge causes massive degradation of hepatic mitochondrial DNA in mice.

Gastroenterology 1999;117:181-90.

22. Krahenbuhl S, Talos C, Fischer S, Reichen J Toxicity of bile acids on the electron transport chain of isolated rat liver mitochondria. Hepatology 1994;19:471-9.

23. Copple BL, Jaeschke H, Klaassen CD. Oxidative stress and the pathogenesis of cholestasis. Semin Liver Dis 2010;30:195-204.

24. Poli G. Pathogenesis of liver fibrosis: role of oxidative stress. Mol Aspects Med 2000;21:49-98.

25. Owen OE, Reichle FA, Mozzoli MA, Kreulen T, Patel MS, Elfenbein IB, et al. Hepatic, gut, and renal substrate flux rates in patients with hepatic cirrhosis. J Clin Invest 1981;68: 240-52.

26. The French METAVIR Cooperative Study Group. Intraobserver and interobserver variations in liver biopsy interpretation in patients with chronic hepatitis C. Hepatology 1994;20:15-20.

27. Bedossa P, Poynard T. An algorithm for the grading of activity in chronic hepatitis C. The METAVIR Cooperative Study Group. Hepatology 1996;24:289-93.

28. Kim SY, Seok JY, Han SJ, Koh H. Assessment of liver fibrosis and cirrhosis by aspartate aminotransferase-to-platelet ratio index in children with biliary atresia. J Pediatr Gastroenterol Nutr 2010;51:198-202.

29. Ramos A, Santos C, Alvarez L, Nogues R, Aluja MP. Human mitochondrial DNA complete amplification and sequencing: a new validated primer set that prevents nuclear DNA sequences of mitochondrial origin co-amplification. Electrophoresis 2009;30:1587-93.

30. Rothberg JM, Hinz W, Rearick TM, Schultz J, Mileski W, Davey M, et al. An integrated semiconductor device enabling non-optical genome sequencing. Nature 2011;475:348-52.

31. Ruiz-Pesini E, Lott MT, Procaccio V, Poole JC, Brandon MC, Mishmar D, et al. An enhanced MITOMAP with a global mtDNA mutational phylogeny. Nucleic Acids Res 2007;35:823-8.

32. Fan L, Yao YG. MitoTool: a web server for the analysis and retrieval of human mitochondrial DNA sequence variations. Mitochondrion 2011;11:351-6.

33. Medina J, Moreno-Otero R. Pathophysiological basis for antioxidant therapy in chronic liver disease. Drugs 2005;65:2445-61.

34. Hartley JL, Davenport M, Kelly DA. Biliary atresia. Lancet 2009;374:1704-13.

35. Zeharia A, Friedman JR, Tobar A, Saada A, Konen O, Fellig Y, et al. Mitochondrial hepato-encephalopathy due to deficiency of QIL1/MIC13 (C19orf70), a MICOS complex subunit. Eur J Hum Genet. 2016 Aug 3. Available from: http://www.ncbi.nlm.nih.gov/pubmed/27485409 [Epub ahead of print]

36. Schroder T, Kucharczyk D, Bar F, Pagel R, Derer S, Jendrek ST, et al. Mitochondrial gene polymorphisms alter hepatic cellular energy metabolism and aggravate diet-induced non-alcoholic steatohepatitis. Mol Metab 2016;5:283-95.

37. Guy J, Qi X, Pallotti F, Schon EA, Manfredi G, Carelli V, et al. Rescue of a mitochondrial deficiency causing Leber Hereditary Optic Neuropathy. Ann Neurol 2002;52:534-42.

38. Ugalde C, Hinttala R, Timal S, Smeets R, Rodenburg RJ, Uusimaa J, et al. Mutated ND2 impairs mitochondrial complex I assembly and leads to Leigh syndrome. Mol Genet Metab 2007;90:10-4.

39. Burman JL, Itsara LS, Kayser E-B, Suthammarak W, Wang AM, Kaeberlein M, et al. A Drosophila model of mitochondrial disease caused by a complex I mutation that uncouples proton pumping from electron transfer. Dis Model Mech 2014;7:1165-74.

ABSTRACT (IN KOREAN)

담도폐쇄증에 의한 담즙 정체성 간질환에서의 미토콘드리아 유전자 돌연변이 연구

<지도교수 박 국인>

연세대학교 대학원 의학과

고 홍

담도폐쇄증은 특징적으로 담즙 배설을 위한 간외 담도의 폐쇄로 인해 발행하는 심각한 담즙 정체성 질환이다. 진단 이후 이를 치료하기 위해 카사이 수술을 신속하게 시행하게 되나 안타깝게도 일부의 환자에게서는 성공적인 수술 이후에도 간 기능의 손상이 점차 진행되는 것을 관찰할 수 있다. 이와 같이 적절한 수술적 치료를 시행함에도 불구하고 이후로 진행되는 간 손상은 현재 간세포내의 미토콘드리아 DNA의 돌연변이와 이로 인한 미토콘드리아의 기능 장애와 깊은 관련이 있을 것으로 생각되고 있다. 이와 같은 간내 미토콘드리아 기능 이상의 임상적 추측에 대한 실험적 접근을 위해 본 연구는 대조질환군으로서 5명의 총담관낭 환자와 환자군으로서 14명의 담도폐쇄증 환자로부터 각각 획득한 간 조직에서 간세포 미토콘드리아 DNA를 추출하고 미토콘드리아

호흡연쇄 구조의 염기서열을 차세대 염기서열분석법을 이용하여 비교 분석하였다. 결론적으로 본 연구에서는 미토콘드리아 호흡연쇄 구조 유전자 지역에서 아미노산 치환을 수반한 비동의 변이를 관찰하였다. 특히 담도폐쇄증 환자에서 특징적으로 미토콘드리아의 기능에 매우 중요한 하부단위 조립과 양성자 펌프 활성이 포함된 미토콘드리아 호흡연쇄복합체 I 유전자 지역에서 의미 있는 돌연변이를 발견하였다. 또한 발견된 미토콘드리아 유전자 변이를 바탕으로 담도폐쇄증 환자의 간 손상 및 간기능 손상이 동시에 관찰된 환자군에서 공통적으로 발견된 미토콘드리아 DNA 돌연변이(T119A, I278V in ND2 of complex I)와 간 손상 없이 간기능 손상만 관찰되었던 환자군에서 공통적으로 발견된 미토콘드리아 DNA 돌연변이(Y95H, S95stop in ND4 of complex I)가 간질환의 임상양상과 의미 있게 관련되고 있음도 확인하였다. 따라서 본 연구는 정상적인 간 세포 생리활성에서 미토콘드리아의 역할이 중요함을 강조함과 동시에 담도폐쇄증에서 성공적인 수술 이후 일부에서 발생하는 간기능 악화를 위시한 병리적인 질병 경과를 미토콘드리아의 기능 이상으로 충분히 설명할 수 있을 것으로 판단된다.

핵심되는 말: 담도폐쇄증, 미토콘드리아 DNA 돌연변이, 호흡 연쇄 복합체, 차세대 염기서열분석법